N95-14478

RECENT ADVANCES IN THE MODELLING OF CRACK GROWTH UNDER FATIGUE LOADING CONDITIONS

A.U. de Koning and H.J. ten Hoeve
National Aerospace Laboratory NLR
The Netherlands

T.K. Henriksen
European Space Agency, ESTEC
The Netherlands

SUMMARY

Fatigue crack growth associated with cyclic (secondary) plastic flow near a crack front is modelled using an incremental formulation. A new description of threshold behaviour under small load cycles is included. Quasi-static crack extension under high load excursions is described using an incremental formulation of the R-(crack growth resistance)- curve concept.

The integration of the equations is discussed. For constant amplitude load cycles the results will be compared with existing crack growth laws. It will be shown that the model also properly describes interaction effects of fatigue crack growth and quasi-static crack extension.

To evaluate the more general applicability the model is included in the NASGRO computer code for damage tolerance analysis. For this purpose the NASGRO programme was provided with the CORPUS and the STRIP-YIELD models for computation of the crack opening load levels. The implementation is discussed and recent results of the verification are presented.

INTRODUCTION

For over two decades models of fatigue crack growth have been based on empirical laws that relate the amount of crack growth in a load cycle to the stress intensity factor range $\Delta K = K_{max} - K_{min}$ or the effective [1] range $\Delta K_{eff} = K_{max} - K_{op}$. Correction factors were included for near threshold behaviour and accelerated growth in the high K regime.

From a physical point of view such crack growth laws are speculative because crack growth and plastic deformation are irreversible processes that depend on the loading history. By nature, such processes must be described in an incremental way and properly integrated to obtain the amount of crack growth for a load cycle or the part of a load cycle for which the incremental description is valid [2, 3]. Clearly, such a new description allows that a distinction is made between the part of a load range where secondary (cyclic) plastic flow is observed and the part where primary plastic flow developes under monotonic increasing loads. For each of these domains an incremental crack growth law can be formulated. Then after integration over the appropriate load ranges the contributions to the crack growth rate for the load cycle under consideration are obtained. In a

similar way "range pair" (or "rain flow") principles may be used to select the appropriate crack growth equations and associated ranges of applicability. In addition, the incremental formulation allows the introduction of other terms representing time and/or environment dependent crack growth. In these applications the integration of the incremental equations becomes more complicated, however, with the increased capabilities of both the numerical techniques and the new generation of computer systems numerical integration appears to be feasible.

In this paper the formulation of two incremental crack growth laws, one describing fatigue crack growth and a second one for static crack extension, is discussed. For constant amplitude loading the equations are integrated analytically to obtain the crack growth rate per load cycle. The result can be compared with the common crack growth laws and allows the material parameters to be determined from the results of simple fatigue crack growth tests. For more complicated load sequences like block programme loading and arbitrary, cycle by cycle defined sequences, a method for integration of the crack growth rate is discussed. The models and methods were implemented into the NASGRO (ESACRACK) software [4] and thoroughly tested. In view of uncertainties about the values of constraint factors a preliminary verification was executed using some new test results obtained for three materials: a titanium alloy Ti-6Al-4V, the aluminium alloy 7075-T73 and the "COLUMBUS" skin material 2219-T851 for the European space station manned module. Two material thicknesses were involved: 2 or 4 mm sheet and, 10 mm, plate material. The initial precracks were edge cracks, surface cracks and through the thickness cracks. After preliminary verification the models were readjusted and the constraint factors specified in more detail. Some of the proposed modifications are discussed. The final verification also includes a large number of test cases collected from the open literature in addition to in-house test results [5].
This paper describes the status of the study after completion of the preliminary verification and the model evaluation.

THE LOADING AND CRACK GROWTH REGIMES DISTINGUISHED IN THE UPWARD PART OF A LOAD CYCLE

In the upward part of a load cycle different regimes can be distinguished, depending on the characteristics of the plastic deformation behaviour and the state of opening of the crack. To illustrate these domains in figure 1 the loading path is shown in a K versus c plot, where c is the crack length. The different loading regimes are indicated and discussed one after another.

Closed crack regime 1, $K_{min} \leq K < K_{op}$

Starting at the minimum stress intensity factor K_{min} the load is increased until the crack opening level K_{op} is obtained. In this first regime 1, characterized by $K_{min} \leq K < K_{op}$, the crack is at least partly closed and the contact areas on the crack surfaces decrease when the applied load is increased. Although the stress intensity factors in this regime are calculated assuming the presence of the crack, it is clear that the effective loading of the crack tip region is very small and no crack growth is assumed in this regime.

Opened crack but no growth regime 2, $K_{op} \leq K < K_{op} + \delta K_{th}$

At level K_{op} the crack is fully opened, but, it takes another increase by δK_{th} to initiate crack growth. Obviously, some crack tip blunting occurs in this regime 2. Models and empirical equations

for computation of values for K_{op} and δK_{th} are discussed later on.

Fatigue crack growth in regime 3, $K_{op} + \delta K_{th} \leq K < K_*$

Upon a further increase of the applied load crack growth is initiated when the stress intensity factor K exceeds the level $K_{op} + \delta K_{th}$. In this regime 3 alternating secondary plastic flow is observed in a relatively small plastic zone. At level $K = K_*$, however, the cyclic plastic flow is assumed to change to primary plastic flow. This transition is characterized by a discrete jump in plastic zone size and a loss of load history effects on the state of deformation. To describe the crack growth behaviour in regime 3, corresponding to $K_{op} + \delta K_{th} < K \leq K_*$, the following incremental crack growth law is adopted

$$dc = \left[C_1(K-K_{op})^n + C_2\delta K_{th}^p(K-K_{op})^{n-p}\right]dK \tag{1}$$

In this expression the first term on the right hand side is an incremental form of Elber's law. The second one is added to describe threshold effects, if present. The power n-p follows from the requirement that the units of both terms must be the same.
At initiation of crack growth, when, $K = K_{op} + \delta K_{th}$, it follows that

$$\left\{\frac{dc}{dK}\right\}_{th} = \delta K_{th}^n(C_1+C_2) \tag{2}$$

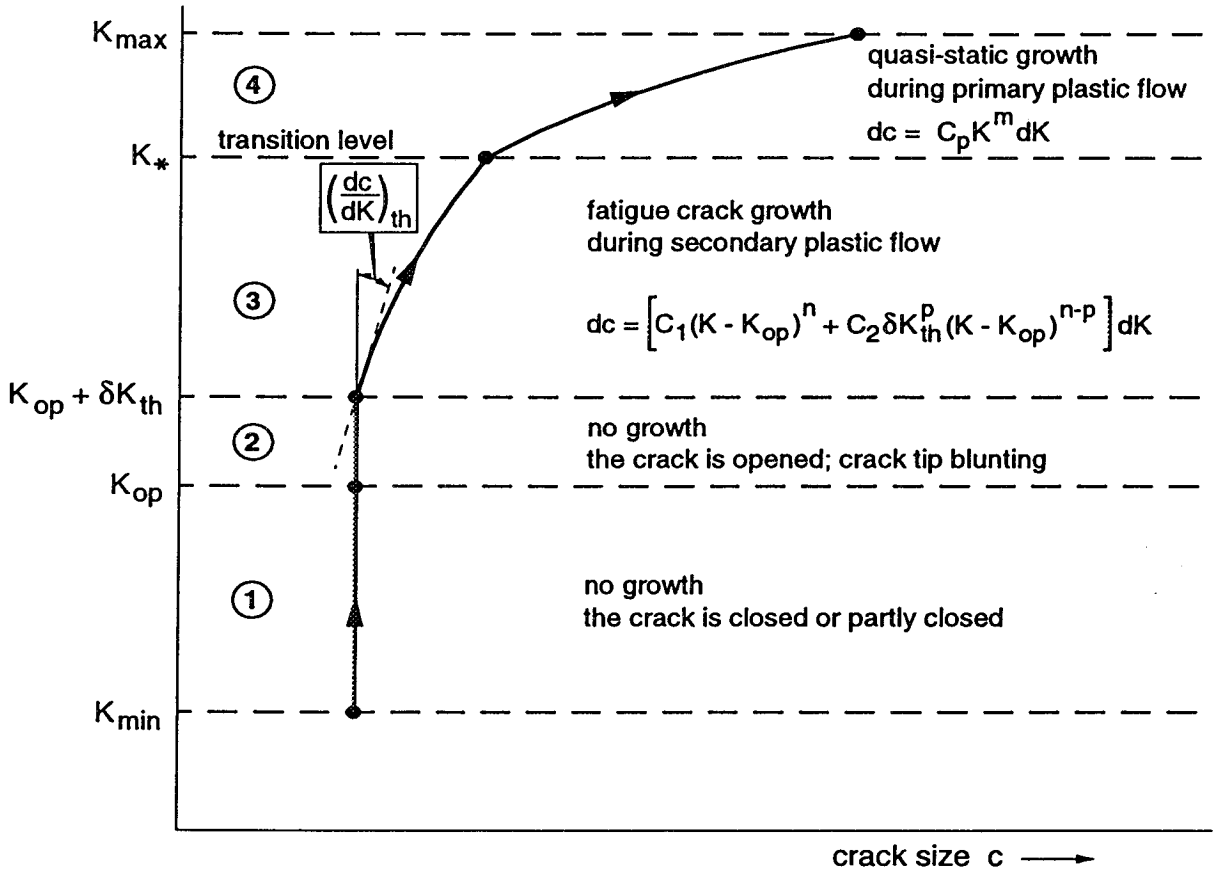

Fig. 1 Different loading and crack growth regimes in one (half) load cycle

Obviously, there exists a relation between the material parameters C_1 and C_2, the threshold level δK_{th} and the slope of the crack growth curve (see Fig. 1). At the present time knowledge about this slope is lacking. Therefore, a convenient value for the slope is selected to simplify the equations. This value is

$$\left[\frac{dc}{dK}\right]_{th} = pC_1\delta K_{th}^{n}/(n+1) \tag{3}$$

To obtain the amount of crack growth Δc_s created under regime 3 the crack growth law (1) must be integrated over the range $K_{op} + \delta K_{th} < K \leq K_*$. There results

$$\Delta c_s = \frac{C_1}{n+1}(K_* - K_{op})^{n+1}\left[1 - \left[\frac{\delta K_{th}}{K_* - K_{op}}\right]^{p}\right] \tag{4}$$

In the next section this equation is used to derive an equation for computation of the transition level K_*. If the transition level is above K_{max} then the upper bound in the integration of eq. (1) is K_{max} and in eq. (4) K_* is substituted by K_{max}.

Quasi-static crack extension regime 4, $K_* \leq K \leq K_{max}$

Loading above the transition level K_* is assumed to induce quasi-static crack extension. In this regime the plastic deformation behaviour takes place under monotonic increasing loads. This implies that the effects of secondary cyclic loading on the actual material behaviour are lost. Thus, the crack opening load and threshold behaviour become insignificant [2, 3]. Moreover, the plastic zone sizes are much greater. To describe crack growth in this domain we will adopt the incremental formulation of the R (or J) curve approach. Assuming small scale plastic behaviour and small amounts of static crack extension the crack growth law adopted is written as

$$dc = C_p K^{m} dK \tag{5}$$

In addition, for cases where wide scale plastic deformation occurs or the amount of static crack extension becomes large we may choose to introduce new -or sub- regimes and formulate the applicable crack growth law in such a way that it describes these processes properly.
The incremental crack growth law must be integrated over the applicable range to obtain the contribution Δc_p to the crack growth increment for a load cycle. There results

$$\Delta c_p = \frac{C_p}{m+1}\left[K_{max}^{m+1} - K_*^{m+1}\right] \tag{6}$$

DETERMINATION OF THE TRANSITION LEVELS K_{op}, $K_{op} + \delta K_{th}$, AND, K_*

The crack opening level, K_{op}

In this study the following crack opening models are used: The mechanical STRIP-YIELD (= modified discretized Barenblatt/Dugdale) model [6, 7, 8, 9] and the empirical CORPUS

(Computation Of Retarded crack Propagation Under Spectrum loading) model [10, 11, 12]. Both models were included in the NASGRO software [4, 5]. In both crack opening models constraint factors are introduced to account for 3D effects on the yield stresses of material in front of the crack tip (in tension and in compression) and the yield stress for loading of material in compression in the wake of the crack. These effects are thought to be determined by the state of stress, the uniaxial yield limit $\bar{\sigma}$ and the sheet or plate thickness T. Only two parameters are considered to be material parameters, namely: the ratio α_{NEW} of the cyclic yield limit in tension over its value in compression, and, the uniaxial yield limit $\bar{\sigma}$. The modelling of the constraint effects will be discussed later on. The STRIP-YIELD model included in NASGRO was derived from the NLR model [7]. Newman's method [13] for computation of the crack opening load from the contact stress solution at the minimum load in the cycle was adopted.
Since in some of the applications the static crack extension plays an important role its effect on the crack opening level K_{op} must be accounted for. In the STRIP-YIELD model this is simulated by unzipping elements in front of the crack tip one after another. In this study unzipping takes place at the minimum load in the cycle (no additional plastic deformation is added to the wake). In the next version of the model, currently under development, the elements are unzipped at the proper stress intensity level. Then, the effect of the additional stretch resulting from static growth of the crack is automatically included.

In an application of the CORPUS model [10] the crack opening level is calculated using the crack opening function $f(R, \alpha_{NEW}, S_{max}/\bar{\sigma})$. This function is chosen in such a way that the STRIP-YIELD analyses results of constant amplitude data are described accurately. The CORPUS model defines a set of rules for selection of the representative load ratio R and the stress level S_{max} from the loading history. In the next version of CORPUS implemented in the NASGRO software the crack opening function will be corrected for the effects of static growth and other improvements of the STRIP-YIELD model. Then, the model can be used to determine the material parameters also for the STRIP-YIELD model in an efficient way.

To illustrate such corrections on the crack opening function the correction accounting for the effect of static crack extension is discussed in a similar way as in reference [8] where a first order approximation was used. Thus, the crack opening level is written as

$$K_{op}/K_{max} = f(R,\alpha_{NEW},S_{max}/\bar{\sigma}) \tag{7}$$

From the result of eq. (7) we can calculate the crack opening load level S_{op} and estimate the fictitious, STRIP-YIELD based, contact area Δc_w near the crack tip at the minimum load level

$$\Delta c_w = c\left[1 - \sin\left[\frac{\pi}{2}\left[1 - \frac{S_{op}-S_{min}}{\sigma_y^c}\right]\right]\right] \tag{8}$$

where σ_y^c is the yield stress of the material in the wake of the crack. Assuming that the contact area is extended by the amount of growth Δc_p it follows for the correction on the crack opening stress that

$$\Delta S_{op} = \frac{2\sigma_y^c}{\pi}\left[\arcsin\left[\frac{c-\Delta c_w}{c}\right] - \arcsin\left[\frac{c-\Delta c_w}{c-\Delta c_p}\right]\right] \quad (9)$$

in eq. (9) c denotes the crack size.

The effective threshold level, $K_{op} + \delta K_{th}$

The effective threshold range δK_{th} is derived from the empirical relation used in the NASGRO software. There results

$$\delta K_{th} = \frac{1 - f(R,\alpha_{NEW},S_{max}/\bar{\sigma})}{1 - R}(K_{th}-K_{min}) \quad (10)$$

where $K_{th} - K_{min}$ represents the NASGRO threshold stress intensity range and $f(R,\alpha_{NEW},S_{max}/\bar{\sigma})$ is the opening function. The threshold value δK_{th} applies to constant amplitude loading of through the thickness cracks. In the applications to part through cracks and to variable amplitude loading the value of δK_{th} is reduced.

The stress intensity factor at transition from cyclic (secondary) plastic flow to primary flow, K_*

To derive an expression for computation of the level K_* at which the transition from secondary plastic flow to primary plastic flow occurs a loading sequence as given in figure 2 is used. The first spike load 1 has created an overload plastic zone and at the time the second spike is applied the crack tip is assumed to be still situated inside this overload plastic zone. In terms of K versus crack length the situation is sketched in figure 3. Then, from a geometrical consideration and the assumption that the transition occurs when the actual primary plastic zone D_* touches the end of the overload plastic zone D_{SP} the following expression can be written

$$c - c_{SP} + \Delta c_s + D_* - D_{SP} = 0 \quad (11)$$

where c is the crack length at initiation of crack growth in the actual overload cycle 2. The secondary crack growth increment Δc_s, given by eq. (4), is a function of K_*.

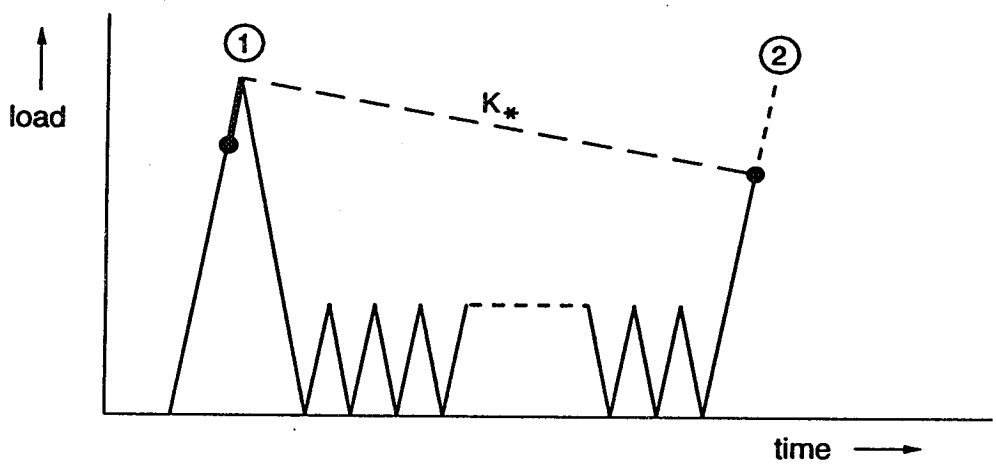

Fig. 2 The loading schedule used to derive an equation for computation of the transition level from secondary to primary plastic flow

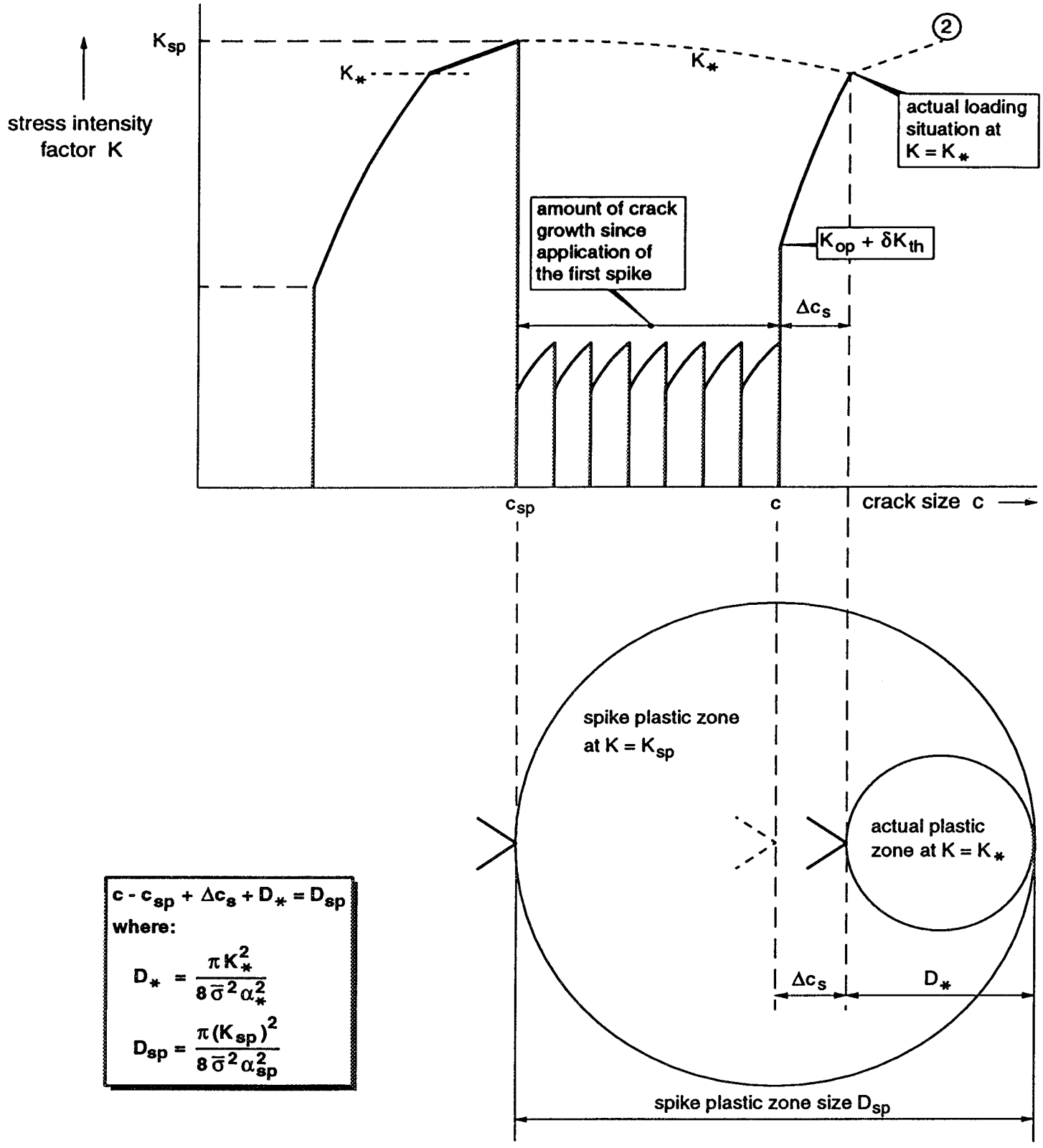

$$c - c_{sp} + \Delta c_s + D_* = D_{sp}$$

where:

$$D_* = \frac{\pi K_*^2}{8\bar{\sigma}^2 \alpha_*^2}$$

$$D_{sp} = \frac{\pi (K_{sp})^2}{8\bar{\sigma}^2 \alpha_{sp}^2}$$

Fig. 3 Geometrical consideration used for determination of the transition level K_*

Further, the plastic zone sizes will be approximated using a first order estimate, that is

$$D_* = \frac{\pi}{8} \frac{K_*^2}{(\alpha_* \bar{\sigma})^2} \tag{12}$$

and

$$D_{SP} = \frac{\pi}{8} \frac{(K_{SP})^2}{(\alpha_{SP} \bar{\sigma})^2} \tag{13}$$

where α_* and α_{SP} are constraint factors introduced to account for 3D effects on the yield stress for primary plastic flow. In the preliminary verification the values α_* and α_{SP} are set equal to the material parameter α_{NEW}. In the next version of the model a more correct description of the constraint behaviour will be introduced. From eqs. (11) to (13), and eq. (4), the value of K_* can be solved in an iterative way. Finally, the value calculated for K_* must be compared with K_{max} in order to establish the presence of primary plastic flow and associated quasi-static crack extension. Primary flow is absent, if $K_* > K_{max}$.

APPLICATION OF THE INCREMENTAL CRACK GROWTH LAWS

Constant amplitude loading

From the foregoing considerations it is concluded that the crack growth rate per load cycle $\Delta c/\Delta N$ can be written as

$$\Delta c/\Delta N = \Delta c_s + \Delta c_p \tag{14}$$

where Δc_s and Δc_p denote respectively the amounts of crack growth associated with secondary plastic flow and with primary plastic flow. After substitution of eqs. (4) and (6) and using the knowledge that in constant amplitude loading $K_{min} \leq K_{op} + \delta K_{th} < K_* \leq K_{max}$ we can calculate $\Delta c/\Delta N$.

In constant amplitude loading K_* is slightly lower than K_{max} in the major part of the crack growth curve. Using this result and recognizing that, in figure 3, c_{SP} can be identified with c eq. (14) can be approximated by

$$\Delta c/\Delta N = C(K_{max}-K_{op})^{n+1} \left[1 - \left(\frac{\delta K_{th}}{K_{max}-K_{op}}\right)^p\right] \left[1 + \left(\frac{K_{max}}{K_{ref}}\right)^{m-2}\right] \tag{15}$$

where $C = C_1/(n+1)$ and the parameter K_{ref} is a combination of the constraint factor α_* and a number of material parameters according to

$$(1/K_{ref})^{m-2} = C_p m \pi (\alpha_* \bar{\sigma})^2/2. \tag{16}$$

In eq. (15) the first part on the right hand side is equal to Elber's crack growth law. The second factor accounts for threshold behaviour in a common way and the third, non-singular, part accounts for static crack extension at higher crack growth rates. Eq. (15) is very similar to common crack growth laws like the NASGRO modified Forman law. This allows the conversion of parameter values by requiring that the different multipliers in eq. (15) have approximately the same effect on $\Delta c/\Delta N$ as the corresponding factors in the crack growth law under consideration. It is concluded here that the incremental description of crack growth has given a physical interpretation of the increased crack growth rate at high K_{max} levels. Further, it is noted that, for any other initial slope of the crack growth curve an expression similar to eq. (15) can be derived.

Constant amplitude loading interrupted at regular intervals for application of a spike load excursion

Relatively large amounts of static crack extension are observed during spike loading excursions applied at regular intervals in an otherwise constant amplitude load sequence, as indicated in figure 4a. Such sequences can be used to determine the material parameter values involved in static crack extension by fitting the integrated crack growth equation to measured data points. In general, an overload ratio OL is chosen of the order 1.5 to 1.7. The number of constant amplitude cycles in one block is in the order of 500 to 2000.

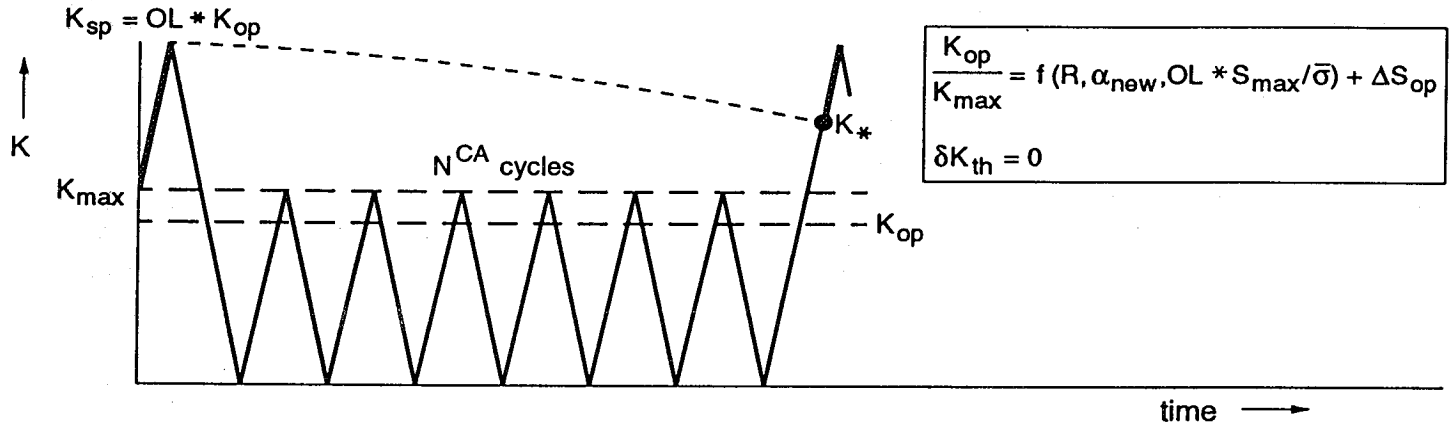

Fig. 4a The spike load sequence for the case, $K_{max} < K_* \leq OL * K_{max}$. (Small N^{CA})

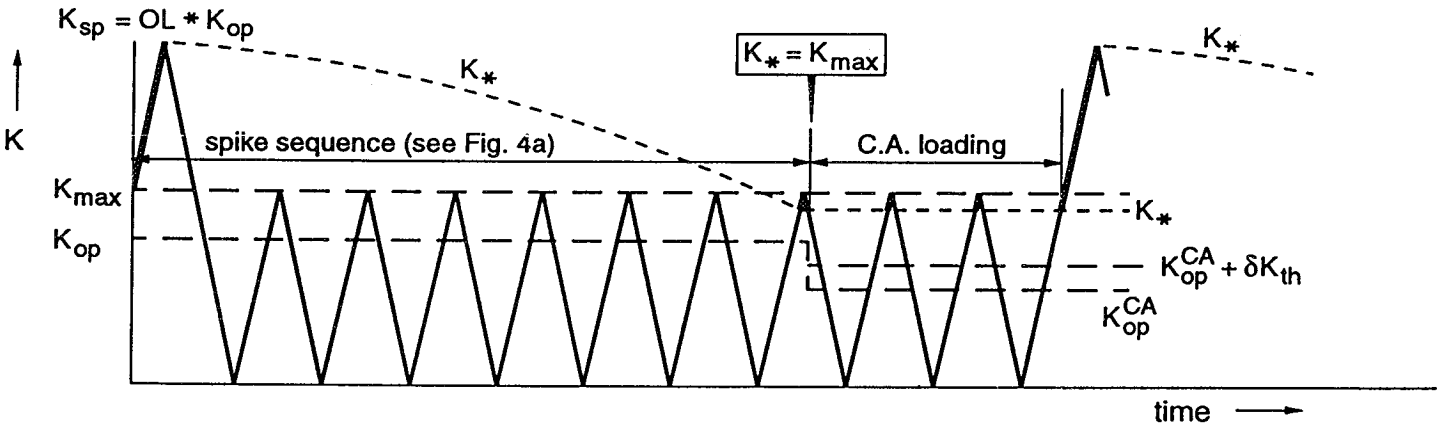

Fig. 4b The spike load sequence for the case of non-interacting spike loads. (Large N^{CA})

C-5.

In such sequences static growth is absent in the constant amplitude cycles provided that $K_{max} < K_* \leq OL * K_{max}$. Thus, the crack growth equation (4) for secondary (cyclic) plastic flow applies to the constant amplitude cycles. For the spike load exclusion K_* must be solved iteratively from eq. (11) and it must be verified that $K_* \geq K_{max}$. Then, it can be derived that the average crack growth rate resulting from application of one block of N^{CA} constant amplitude cycles plus one spike load excursion can be written as

$$\Delta c/\Delta N = \frac{\left[C\left[(K_{max}-K_{op})^{n+1} * N^{CA} + (K_*-K_{op})^{n+1}\right] + \frac{C_p}{m+1}\left[K_{sp}^{m+1} - K_*^{m+1}\right]\right]}{(N^{CA}+1)} \quad (17)$$

where it is assumed that K_{op} is independent on the crack size and can be calculated using the simple crack opening function (7) when S_{max}, α_{NEW}, and R are associated with the spike load cycle.
In the case $K_* \leq K_{max}$ the contribution of static growth of the crack must be calculated. This situation is shown in figure 4b. To calculate the crack growth rate for this part of the constant amplitude cycles eq. (15) can be used. The result can be added to eq. (17) as a weighted average to obtain crack growth rate for one block.
In the applications discussed in this paper the Overload Level OL is chosen to be so high that threshold behaviour is absent, and, $K_* > K_{max}$.

Block programme loading and randomized or cycle by cycle defined load sequences

In the aerospace industry load spectra are often defined as blocks consisting of a number of different load steps each of which containing a distinct number of constant amplitude cycles of a given amplitude and mean load level. In the analysis the load steps can be applied one after another and, using some additional assumptions about the transition from one load step to the next one, we can analyze this specific load sequence derived from the load spectrum (see Fig. 5). Alternatively,

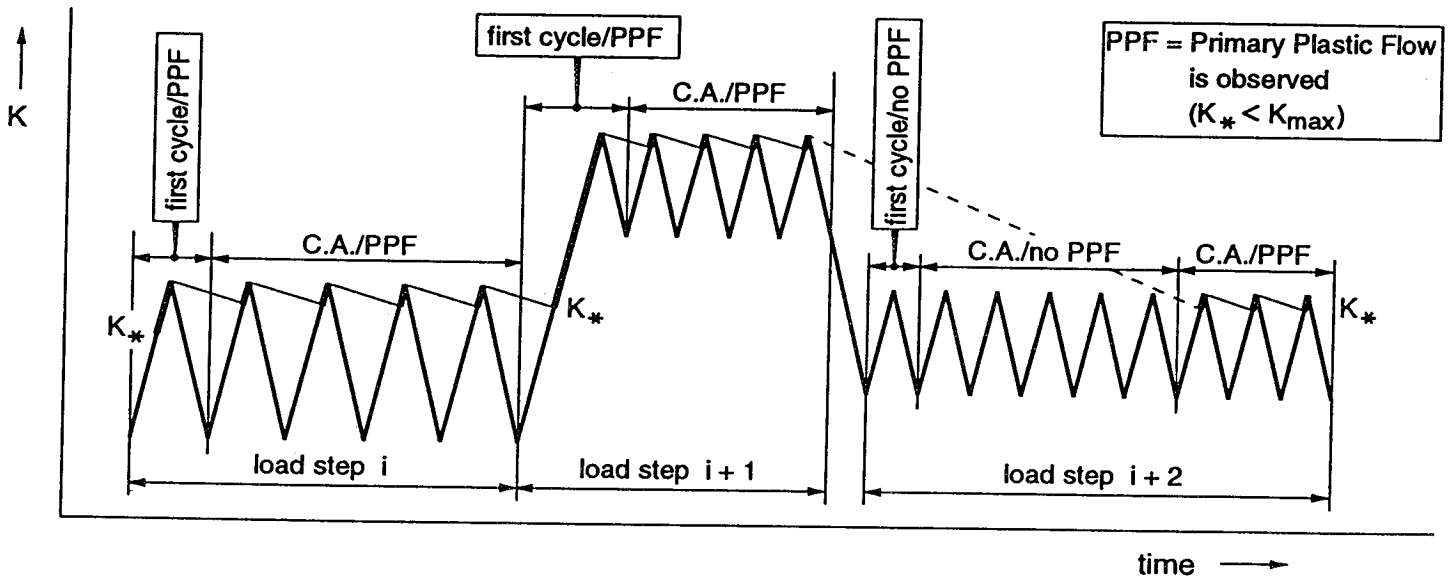

Fig. 5 Three load steps from a block programme load sequence. Parts where crack growth during primary plastic flow (PPF) occurs are indicated. Note the different behaviour in the first cycle of a load step compared to the remaining part of the constant amplitude cycles.

we can randomize the cycles in such a way that, after verification by application of counting methods, the sequence properly represents the load spectrum. In this way different sequences can be constructed all representing the same load spectrum. It is noted, however, that the load sequences do not inevitably represent the same fatigue loading experience.
Characteristic for the aircraft wing and tail load sequences is the presence of air-ground-air load cycles that are included in the load sequence at the proper intervals. In general, these sequences contain many (short) periods of constant amplitude loading that can be described as load steps. Other cycles can also be described as load steps by defining them as single (half) cycles.
In the NASGRO software such a definition of load steps was applied. Each first cycle in a load step is analysed using a separate crack growth prediction module that calculates the crack growth increments Δc_p and Δc_s for that particular cycle.

The remaining constant amplitude cycles are analysed by taking discrete steps Δc and (using mid point integration at $c + \frac{1}{2}\Delta c$) the number of cycles corresponding to the stepsize Δc is calculated and subtracted from the number of cycles left in the load-step. In this way each of the load steps is analysed one after another.

PRELIMINARY VERIFICATION AND MODEL EVALUATION

Model definition

In an application of the crack growth and crack opening models additional assumptions must be made to quantify constraint effects on the yielding and crack opening behaviour.
In an early stage of this study it was decided to execute the preliminary predictions using a highly simplified system of constraint factors. The yield stresses adopted are illustrated in figure 6. The material yield parameter α_{NEW} is accounting for different yielding behaviour of material loaded in tension compared to material yielding in compression. In compression the yield stress for the wake of the crack is assumed to be the same as the yield stress of material in front of the crack tip. All

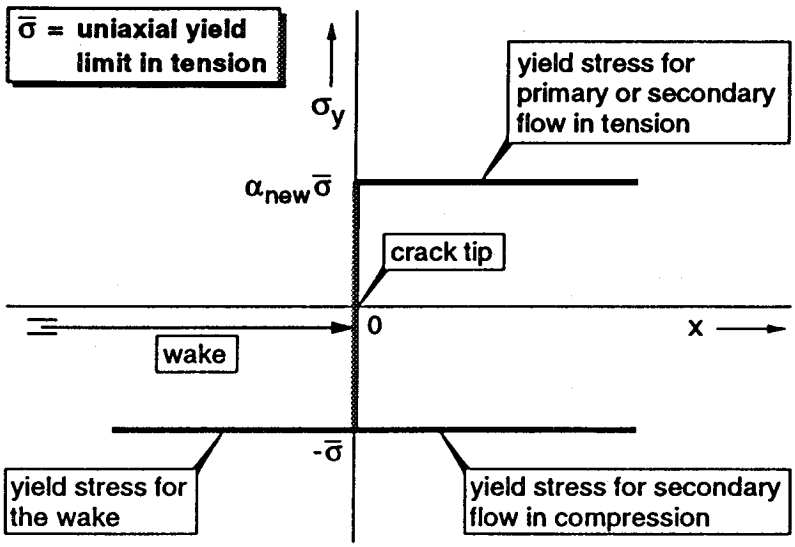

Fig. 6 Yield stresses used for the preliminary predictions

other constraint or Bauschinger effects are assumed to be absent. Later on, after completion and evaluation of the preliminary predictions a more correct definition of constraint factors will be introduced. In the conclusions and discussion some directives are given for such a system. In the application of the CORPUS model the NLR crack opening function is used. The function is given in appendix A.

Test programme

An experimental programme was defined and executed to collect crack growth data for determination of the material parameters in the crack growth law and to verify the models as implemented in the NASGRO software.
The materials involved are Ti-6Al-4V, Al-7075-T73(51) and Al-2219-T851. Both sheet and plate materials are used. The sheet specimens were centrally precracked (through the thickness crack $2c_0 \simeq 6$ mm). The specimen width is 120 mm in all cases. The 10 mm thick plate specimens contained a corner crack or a surface crack. The crack size was 1 mm ($a_0/c_0 = 1$). The load sequences applied in the test are constant amplitude loading at R = 0.05 and R = 0.70, repeated and single spike load sequences and a Space Transportation System STS (pay load) spectrum. The STS spectrum is applied in blocks of constant amplitude loads (full cycles). For the Al-7075-T73(51) material the test programme is given in tables 1a and 1b. For the other two materials a similar test program was executed. As the conclusions drawn from the results of the preliminary verification are the same for all three materials, in this paper the discussions are concentrated on the 7075-T73(51) material. In reference [5] the results obtained for the other materials are discussed in detail.

Table 1a Test programme for 2 mm thick 7075-T73 sheet material. Specimen width is 120 mm

Group	Spec.	Fatigue loading programme	
		Basic loading	Spikes
I	S017075	C.A., R = 0.05, S_{max} = 89.2 MPa	-
	S027075	C.A., R = 0.05, S_{max} = 89.2 MPa	-
II	S037075	C.A., R = 0.7, S_{max} = 282.5 MPa	-
	S047075	C.A., R = 0.7, S_{max} = 282.5 MPa	-
III	S057075	C.A., R = 0.05, S_{max} = 89.2 MPa	S_{sp} = 151.6 MPa, ΔN = 500 cycles
	S067075	C.A., R = 0.05, S_{max} = 89.2 MPa	S_{sp} = 151.6 MPa, ΔN = 1000 cycles
	S077075	C.A., R = 0.05, S_{max} = 89.2 MPa	S_{sp} = 151.6 MPa, ΔN = 2000 cycles
	S087075	C.A., R = 0.05, S_{max} = 89.2 MPa	S_{sp} = 151.6 MPa at c = 5, 7, 10 mm
IV	S117075	C.A., R = 0.05, S_{max} = 101.1 MPa	S_{sp} = 151.6 MPa at c = 5, 7, 10 mm
	S147075	C.A., R = 0.05, S_{max} = 101.1 MPa	S_{sp} = 151.6 MPa, ΔN = 2000 cycles
V	S127075	STS spectrum, S_{max} = 151.6 MPa	-
	S137075	STS spectrum, S_{max} = 282.1 MPa	-

Table 1b Test programme for 10 mm thick 7075-T7351 sheet material. Specimen width is 50 mm

Group	Spec.	Type of notch	Fatigue loading programme	
			Basic loading	Marker loading or spikes
A	P017075	SC	C.A., R = 0.05, S_{max} = 135 MPa	Marker loading: C.A., R = 0.6 S_{max} = 66.8 Mpa at c = 5, 7.5, 10, 13 mm
B	P027075	SC	C.A., R = 0.05, S_{max} = 135 MPa	S_{sp} = 229.5 MPa, ΔN = 2000 cycles
	P077075	SC	C.A., R = 0.05, S_{max} = 135 MPa	S_{sp} = 229.5 MPa at c = 5, 7, 10 mm
	P047075	CC	C.A., R = 0.05, S_{max} = 135 MPa	S_{sp} = 229.5 MPa, ΔN = 2000 cycles
C	P057075	SC	C.A., R = 0.05, S_{max} = 153 MPa	S_{sp} = 229.5 MPa at c = 5, 7, 10 mm
	P087075	CC	C.A., R = 0.05, S_{max} = 153 MPa	S_{sp} = 229.5 MPa, ΔN = 2000 cycles
D	P067075	SC	STS spectrum, S_{max} = 340 MPa	-

c = half crack length along specimen surface
SC = Surface Crack
CC = Corner Crack

Determination of the material parameters

The material parameters appearing in the crack growth laws (4) and (15) can be determined by minimizing the distances of the measured data points to the plotted graph of the crack growth equation in the log $\Delta K = K_{max} - K_{min}$ versus log (da/dN) domain. From the test matrix defined for centrally cracked sheet specimens the following tests were chosen for determination of the material parameters:

S017075 Constant amplitude loading at R = 0.05.
S037075 Constant amplitude loading at R = 0.70.
S067075 Constant amplitude loading, interrupted each 1000 cycles for application of a spike load. The spike load ratio S_{SP}/S_{max} = 1.7. The load ratio R = 0.03 (for the spike).

The test results obtained for these 3 tests are collected in one series of dc/dN(i) - ΔK(i) data sets. Then, using a standard routine the parameter values in the crack growth law are determined in an iterative way such that

$$\text{sum} = \sum_i \left[\ln(dc/dN(i)) - \ln F(\Delta K(i), K_{op}(i), S_{max}, R) \right]^2 \qquad (18)$$

is a minimum. Thus, the least squares fit is applied on a log scale. In eq. (18) function F(ΔK(i), K_{op}(i), S_{max}, R) represents the right hand side of the crack growth law eq. (15) for S017075 and S037075. In the evaluation of test S067075, eq. (17) is used to calculated the average crack growth rate.

The crack opening loads $K_{op}(i)$ and, therefore, the values of the material parameters in F depend on the crack opening model that is chosen. In the determination of the material parameters the CORPUS model is applied in combination with the NLR opening function. A complicated iterative scheme based on a STRIP-YIELD analysis of $K_{op}(i)$ was thought to be impractical. The "fit" results are indicated in figure 7b. For comparison the fit results obtained for Ti-6Al-4V and Al-2219-T851 are given in figures 7a and 7c. From figure 7 it is concluded that the data of the constant amplitude load sequences (S01 and S03) are described properly. The spike load sequence (S06) is more difficult. In the lower ΔK regime the crack growth rate is underestimated by the CORPUS model. At higher ΔK Levels the contribution of the primary plastic flow component to the crack growth rate is described in a correct way [14] and the value for the yield parameter α_{NEW} in this study can be determined.
Clearly, the addition of the spike load sequence to the constant amplitude sequences helps to determine a useful value for α_{NEW}. Further, it is noted that the more common non-retardation models for crack growth prediction can not predict a lower crack growth rate for case S06 compared to S01. The contribution of the spikes will slightly increase the crack growth rate in these models. From figure 7, however, it can be seen that the crack opening models predict a crack growth rate that is one order of magnitude lower (case S06) compared to case S01. This agrees with the test results.

The values obtained for the material parameters are shown in table 2. Other material properties are given in reference [5]. The corresponding values of parameters in the NASGRO crack growth law [4] were determined by fitting the same data points. In this case the parameters q and K_c are thought to represent the static crack growth properties; values for these two parameters are calculated directly from m and K_{ref} in the incremental crack growth model discussed here. Further, the threshold parameter is kept at the same value, so, in this case the fit parameters are C, n, p and α_{NEW}. In sequence S06 the contribution of static growth due to the spikes is accounted for in the same way as described for the incremental crack growth law. The parameter values obtained are shown in table 3.

Table 2 Material parameter values determined for the incremental crack growth law discussed in this study (in MPa, mm)

	7075-T73	Ti-Al-4V	2219-T851
Elber coefficient C	0.276E-10	0.294E-10	0.32527E-10
Elber exponent n+1	2.999	2.656	2.895
Threshold exponent p	1.36	5.955	5.948
Threshold level ΔK_{th}	87.49	506.28	249.20
Static growth exponent m	17.64	10.06	12.99
Static growth parameter K_{ref}	1945.2	4427.2	1889.4
Yield parameter α_{NEW}	1.053	1.197	1.24

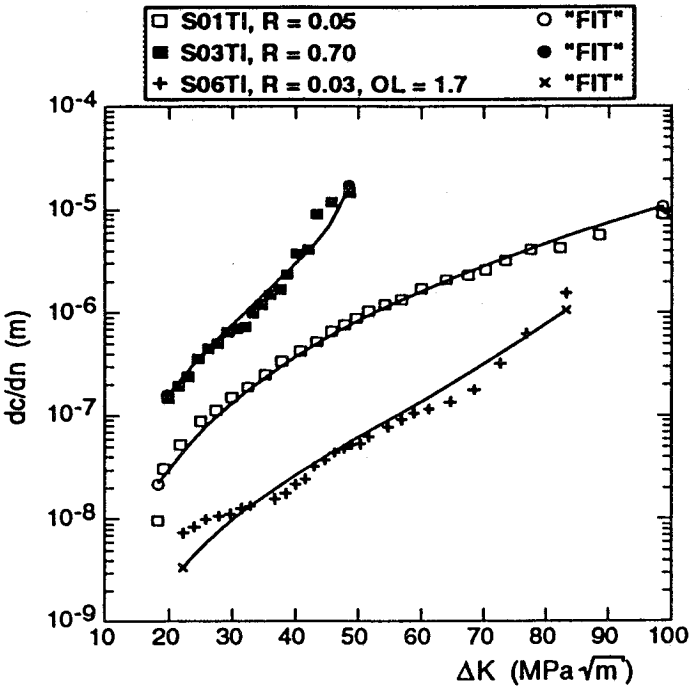

Fig. 7a Plot of the crack growth equation fitted to the measured data points. The material is Ti-6Al-4V. The thickness is 2 mm.

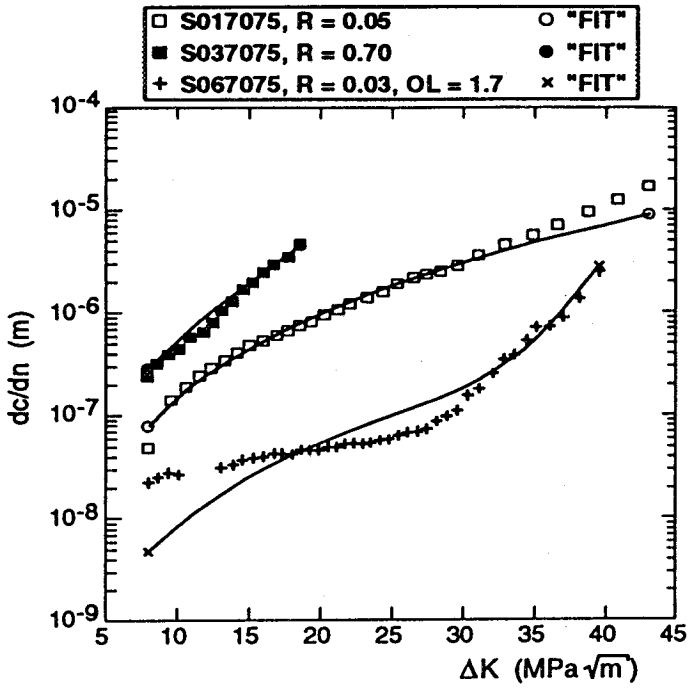

Fig. 7b Plot of the crack growth equation fitted to the measured data points. The material is 7075-T7351. The thickness is 2 mm.

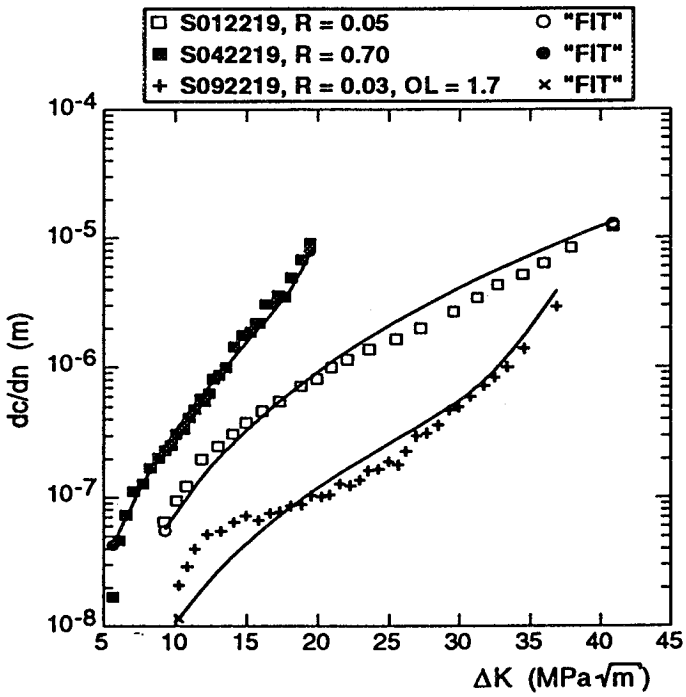

Fig. 7c Plot of the crack growth law fitted to the measured data points. The material is 2219T851. The thickness is 2 mm.

Table 3 Material parameter values determined for the NASGRO modified Forman crack growth law (MPa, mm)

	7075-T73	Ti-Al-4V	2219-T851
Elber coefficient C	0.1745E-9	0.2621E-10	0.135E-10
Elber exponent n	2.657	2.656	3.399
Threshold exponent p	1.150	0.113	0.100
Threshold level ΔK_{th}	87.49	506.28	249.20
Static growth exponent q	0.208	0.382	0.213
Critical K_c	2063.30	5254.92	2040.89
Yield parameter α_{NEW}	1.049	1.199	1.358

Results obtained for the sheet specimens

Using the NAGRO programme and the values of the material parameters from table 3 the crack growth rates and crack size were predicted. The results are collected in figures 8 and 9. Each plot represents one test case that includes the experimental result and the result predicted by the CORPUS and the STRIP-YIELD models. The first symbol in the identification indicates the type of material (Sheet or Plate). The next digits give, the sequence number of the test and the rest identifies the material.

Comparison of dc/dN versus c data (Figs. 8a and 8b)

The data sets used for the determination of the material parameter values were S017075, S037075 and S067075. From the corresponding plots it is seen that the "fit" results are reproduced properly by the CORPUS and by the STRIP-YIELD modules in NASGRO. This justifies the use of the CORPUS crack opening model for determination of the material parameters. The rather strong deviations observed for smaller crack sizes in the S05, S06 and S07 spike load tests are probably due to the simple definition of the constraint parameters. The same applies to all crack sizes for the relatively low spike level in test S14. It appears that too much plastic deformation is predicted by

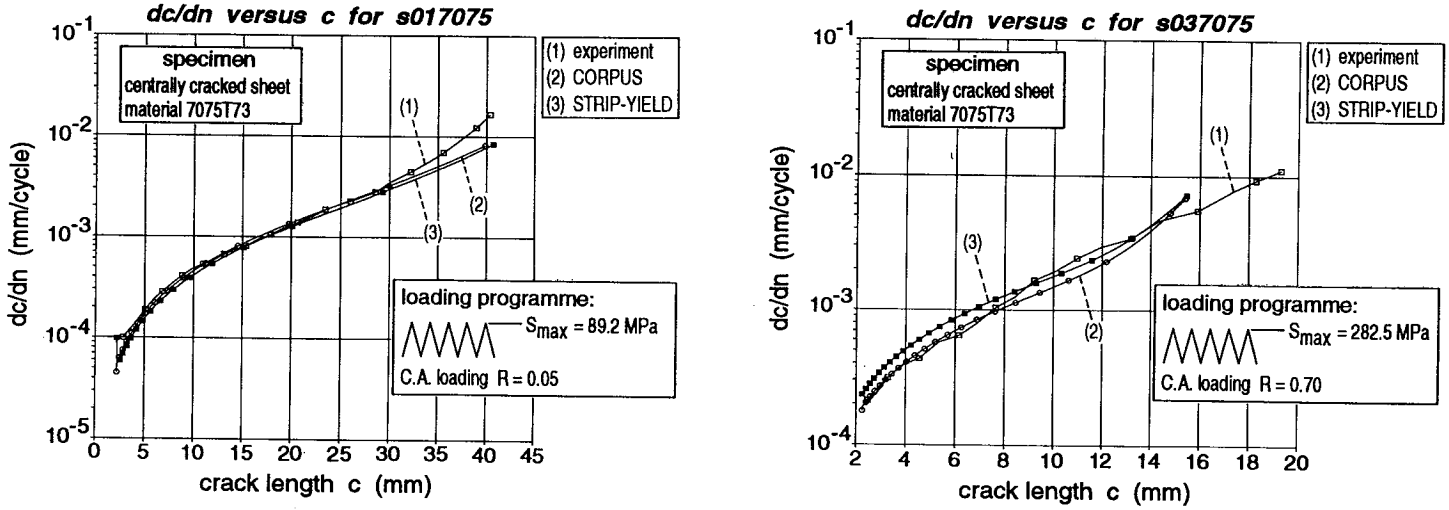

Fig. 8a Comparison of measured and predicted crack growth rates, SHEET specimens

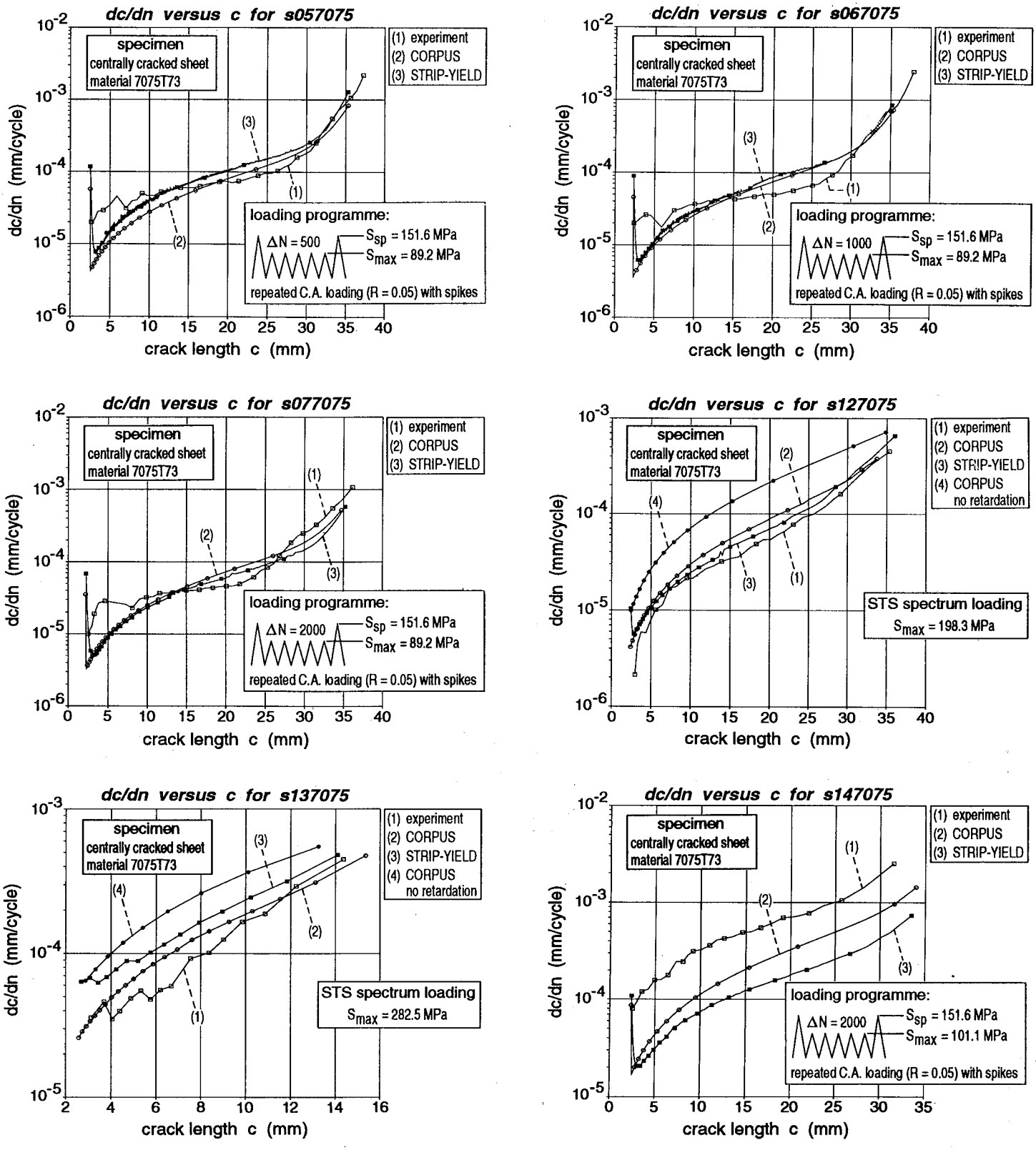

Fig. 8b Comparison of measured and predicted crack growth rates, SHEET specimens (continued)

the STRIP-YIELD model. So, the constraint effect on yielding in secondary flow in tension is underestimated. In constant amplitude loading without spikes this effect is absent. The data predicted by the STRIP-YIELD model for constant amplitude loading at R = 0.70 are based on a cycle by cycle analysis. This guarantees that the contact area at the minimum load is properly modelled (this area is of the same order of magnitude as the element size applied in front of the crack tip).
In general, the first cycle of the load sequences shows a different crack growth rate. This is caused by the model used to predict growth during primary plastic flow. The deviations disappear if the average values for the crack growth rate are plotted in stead of the values per load cycle. It is also observed that the STRIP-YIELD results show some transient behaviour at the beginning of the curves. The CORPUS model does not account for such effects. The interval between two measured data points was to large to see a similar behaviour in the tests.

The three times repeated single spike sequences, S08 and S11, were included in the test program to verify the effect of constraint on the retardation region. As this should be judged in a c versus N plot these results are discussed in the next section.

The behaviour of the specimens subjected to the STS load spectrum (S13) are also shown. The differences are fairly large. The origin of the differences is unknown. For comparison the results obtained for a non-retardation model are also presented.

From the results discussed so far it is concluded that the definition of the constraint factors needs improvement. Further, an increased value of the constraint factor for secondary plastic flow in tension must be used. This will certainly improve the accuracy of the spike load cases as for smaller crack sizes the predicted crack growth rates will increase. For larger crack sizes the effect will diminish compared to the contribution of static crack extension to the crack growth rate. In view of these observations a judgement on the basis of crack size versus number of cycles would be cripple as the deviations observed for the smaller crack sizes will govern the whole picture. For this reason this judgement is postponed until the constraint problems are solved in a satisfactory way.

Comparison of c versus N data (Fig. 9)

The results obtained for the sheet specimen subjected to three single spikes are given in

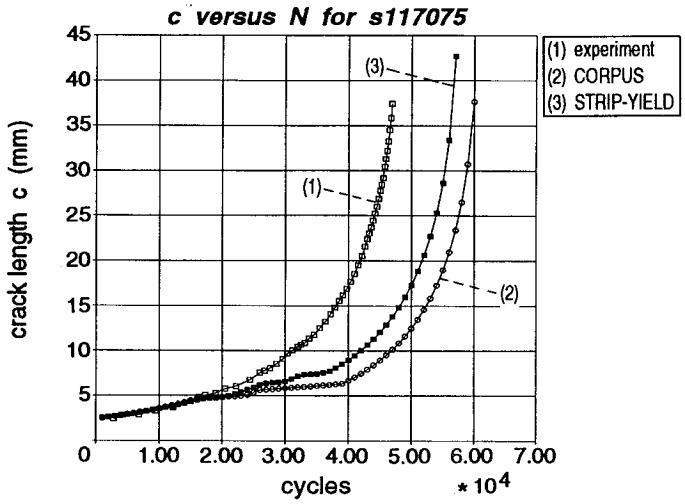

Fig. 9 Comparison of measured and predicted crack growth curves. SHEET specimen subjected to C.A. loading and three single spike loads

figure 9. It is seen that the predicted effects of overloads on the crack growth rate is overestimated. The 1.5 overload level (S11) gives less retardation and, as a result, all curves are more close to the case of constant amplitude loading. The spike loads are applied at approximately the same number of load cycles as used in the experiment. This implies that the crack sizes (and K factors) are smaller and so the plastic zone size and retardation region. As most of the spikes are applied at crack sizes smaller than 10 mm (pure plane stress conditions not yet present) it must be concluded that under plane strain conditions the constraint factor α is higher than assumed in the models. The results obtained for specimen S08 were out of range. These results are left out of the discussion. It is noted that predictions based on linear models do not show any retardation.

Results obtained for the plate materials

Comparison of dc/dN versus c data (Fig. 10a and 10b)

The predictions for the plate material are based on the same material parameter values as used for the sheet specimens. By nature, the influence of bending stresses induced by clamping the thick specimens is more pronounced than for the case of sheet specimens. This may explain part of the larger differences in results obtained for the plate specimens.

For the spike load sequences the conclusion can be drawn that the crack opening load is too high. As mentioned previously this indicates that too much plastic deformation occurs in the constant amplitude cycles and gives support to the introduction of an increased value for the constraint factor for secondary cyclic plastic flow in tension.

The prediction of the specimen under STS spectrum loading is conservative. Further, the deviations between the CORPUS and the STRIPY predictions are relatively large. The source is unknown. Again, it is concluded that the definition of the constraint factor α needs reconsideration.

Comparison of c versus N data (Fig. 11)

The behaviour observed for the single spikes applied three time on the plate specimens is shown in figure 11. The following conclusions can be drawn. The agreement between measured data points and predictions is good for the 1.5 overload cases (P05). For the 1.7 spike load case the predicted delay is far to large for the case (P05), indicating that the constraint factor α must have a higher value to reduce the plastic zone size and the retardation region.

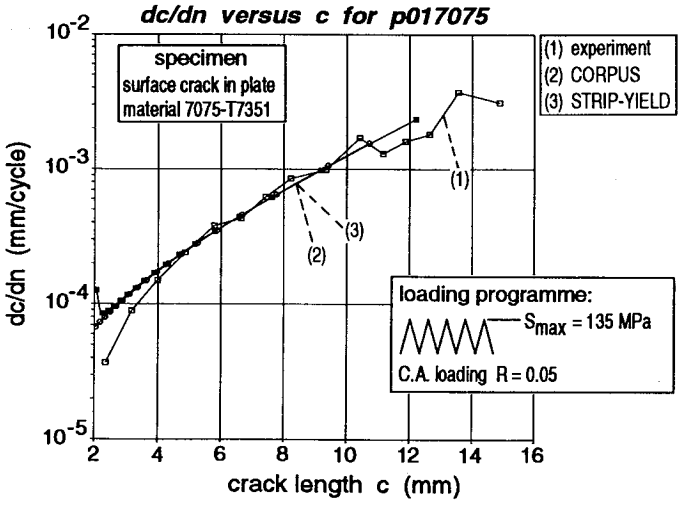

Fig. 10a Comparison of measured and predicted crack growth rates. PLATE specimen

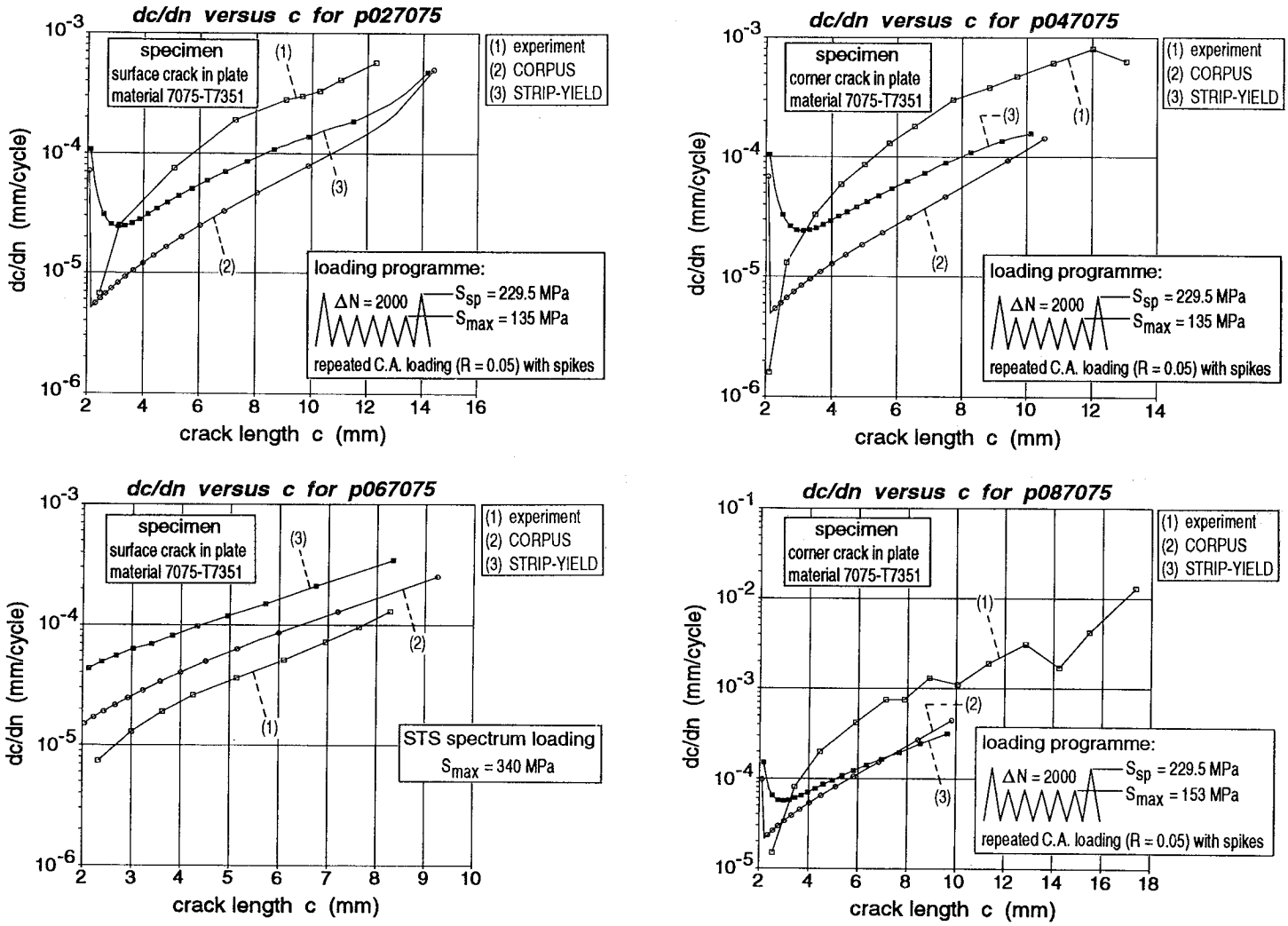

Fig. 10b Comparison of measured and predicted crack growth rates, PLATE specimens (continued)

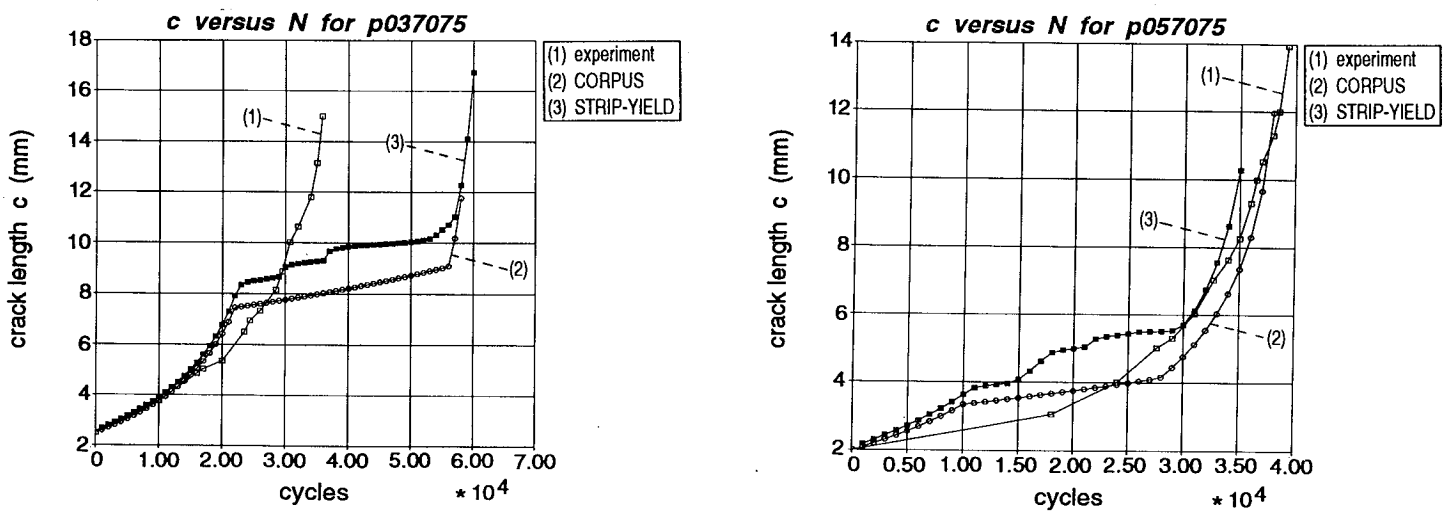

Fig. 11 Comparison of measured and predicted crack growth curves, PLATE specimens

CONCLUSIONS AND RECOMMENDATIONS FOR FURTHER STUDY

1. The empirical CORPUS model and the mechanical STRIP-YIELD model for prediction of the crack opening load level were designed and implemented in the NASGRO software to yield the NASGRO-STRIPY-93 software. This software was tested successfully.

2. Material parameter values were determined successfully using two constant amplitude load sequences executed respectively at R values of 0.70 and 0.05. In addition a repeated spike load sequence was introduced to determine the value of the yield parameter α_{NEW} and the parameters involved in static crack extension during primary plastic flow. For all three materials, Ti-6Al-4V (t = 2 mm), 7075-T73(51) (t = 2 mm) and 2219T851 (t = 4 mm) the material parameters were determined.

3. The model used to describe threshold behaviour under variable amplitude loading is sufficiently accurate. In eq. (1) the threshold parameter C_2 is still to be determined. Further research is recommended.

4. The model introduced to describe accelerated crack growth during primary plastic deformation in virgin material describes the high crack growth rates observed at high K_{max} levels in a satisfactory way. The iterative scheme for computation of the transition levels K_* appears to be functioning properly.

5. It is important to note that constraint effects primarily depend on the state of stress and, therefore, on the loading history, as such a discussion in terms of material parameters is not very useful.

6. The definition and quantification of constraint factors need further improvement. The best way to proceed is to collect and evaluate full 3D Finite Element analyses results of the elastic-plastic deformation and crack growth problem. These are not yet available in sufficient detail. For the time being we need engineering judgement and empirical methods to proceed.

7. The results obtained for constant amplitude loading (cases S01, S03 and P01) are covering states of stress ranging from plane strain to plane stress conditions. This indicates that in constant amplitude loading the crack opening level primarily depends on the yield ratio parameter α_{NEW}. The results obtained for constant amplitude loading interrupted for application of single spikes indicate that under plane strain conditions the yield stresses in tension are much higher than assumed in this study (the value of α_{NEW} appears to be independent of the state of stress). Thus, the constraint system depends on the state of stress. In addition the transition from plane strain to plane stress must be modelled. This can be done in a way as described in references [9] and [11].

8. It is not likely that the constraint effects at different locations in the wake of the crack (resulting from residual stresses) are the same as the constraint effects active in yielding in compression in front of the (closed) crack. Measurement of the residual stresses on the fracture surface is strongly recommended to quantify these constraint effects.

9. The results of this verification indicate that the accuracy of the CORPUS model is close to the accuracy of the STRIP-Yield model in its current formulation. However, the possibility to improve the description of constraint effects gives the STRIP-YIELD model the potential to be superior compared to the empirical CORPUS model. Further, compared to the common non-retardation models for crack growth prediction a better description of the behaviour observed for spike load sequences is demonstrated for both the CORPUS and the STRIP-YIELD models.

ACKNOWLEDGEMENTS

The authors gratefully acknowledge M. Richmond (ARL) for the software development support during the period he worked at NLR, and L. Schra for his efforts to obtain and evaluate the experimental results. The incremental crack growth model was developed under contract no. 1823 with the Netherlands Agency for Aerospace Programs (NIVR). The other work reported in this paper was performed under contract no. 9691 with the European Space Agency (ESA).

REFERENCES

1. Elber, W., The significance of fatigue crack closure. ASTM STP486, 1971, pp. 230-242.

2. Koning, A.U. de, Dougherty, D.J., Prediction of low and high crack growth under constant and variable amplitude loading. Proc. of the spring meeting on "Fatigue crack growth under variable amplitude loading", ed. J. Petit, Paris, 1988.

3. Dougherty, D.J., Koning, A.U. de , and Hillberry, B.H., Modelling high crack growth rates under variable amplitude loading, *Advances in Fatigue Lifetime Predictive Techniques* ASTM STP 1122, 1992, pp. 214-233.

4. Fatigue crack growth computer program "NASA/FLAGRO" version 2.0. JSC-22267 A, Jan 1993, Draft.

5. Koning, A.U. de., Advanced Tools for life prediction and damage tolerance analyses, Contract Report NLR CR 93523 L, 1993.

6. Newman, J.C. Jr., A crack closure model for predicting fatigue crack growth under aircraft spectrum loading, ASTM STP 748, 1981, pp. 53-84.

7. Koning, A.U. de, Liefting, G., Analysis of crack opening behaviour by application of a discretised STRIP-YIELD model, ASTM STP 982, 1988, pp. 437-458.

8. Newman, J.C., Poe, C.C., Dawicke, D.S., Proof test and fatigue crack growth modeling on 2024T3 aluminium alloy, Proc. of Fatigue 90, July 1990.

9. Wang, G.S., Blom, A.F., A modified Duydale-Barenblatt model for fatigue crack growth predictions under general load conditions FFA TN 1987-79, Stockholm, 1987.

10. Koning, A.U. de., A simple crack closure model for prediction of fatigue crack growth rates under variable-amplitude loading. ASTM STP 743, 1981, pp. 63-85.

11. Koning, A.U. de, Linden, H.H. van der., Prediction of fatigue crack growth rates under variable loading using a simple closure model, Proc. of the 11th ICAF Symposium in the Netherlands, 1981 (also NLR MP 81023).

12. Padmadinata, A.H., Investigation of crack-closure prediction models for fatigue in Aluminium Alloy sheet under flight-simulation loading. Thesis, March 27th 1990, Technical University Delft.

13. Newman, J.C., FASTRAN-II- A fatigue crack growth structural analysis program. NASA TM 104159, Febr. 1992.

14. Schijve, J., Fundamental aspects of predictions on fatigue crack growth under variable-amplitude loading. Proc. of "Theoretical concepts and numerical analyses of fatigue". ed. A.F. Blom and C.J. Beevers, EMAS, Birmingham, 1992, pp. 111-130.

APPENDIX A The NLR/CORPUS crack opening function

The crack opening function $f(\alpha_{NEW}, R, S_{max}/\bar{\sigma}) = \frac{S_{op}}{S_{max}}$ is defined in the following way:

$$f = 1 - \alpha_{NEW} + \alpha_{NEW} * CF1 \qquad 0 < \alpha_{NEW} < 1$$

$$f = \frac{1}{2}\left[\frac{3}{\alpha_{NEW}} - 1\right] CF1 + \frac{3}{2}\left[1 - \frac{1}{\alpha_{NEW}}\right] CF2 \qquad 1 \leq \alpha_{NEW} \leq 3$$

$$f = \frac{3}{\alpha_{NEW}} CF2 + \left[1 - \frac{3}{\alpha_{NEW}}\right] CF3 \qquad \alpha_{NEW} > 3$$

In the current CORPUS module the functions CF are assumed to be the following form:

$$CF1 = (.505 + .18R - .135R^2 + .81R^3 - .36R^4) * Hr \qquad 0 \leq R < 1$$
$$CF1 = (.505 + .18R) * Hr \qquad R < 0$$

$$CF2 = .25 + .06R + 1.13R^2 - .44R^3 \qquad 0 \leq R < 1$$
$$CF2 = .25 + .06R \qquad R < 0$$

$$CF3 = R \qquad 0 \leq R < 1$$
$$CF3 = 0 \qquad R < 0$$

where:

$$Hr = 1 - 0.2(1 - R)^3 \left[\frac{S_{max}}{\bar{\sigma}}\right]^3$$